

Arcsecond scale radio polarization of BL Lacertae objects

C. Stanghellini¹, D. Dallacasa², M. Bondi², and R. Della Ceca³

¹ Istituto di Radioastronomia del CNR, C.P. 141, I-96017 Noto SR, Italy

² Istituto di Radioastronomia del CNR, Via Gobetti 101, I-40129 Bologna, Italy

³ Osservatorio Astronomico di Brera, Via Brera 28, I-20121 Milano, Italy

Received 10 October 1996 / Accepted 22 October 1996

Abstract. We present deep VLA radio observations of six sources from the 1 Jy sample (Stickel et al. 1991) of radio selected BL Lac objects (RBL). The polarization properties of the extended emission of these objects are not consistent with those of the FR I radio galaxies (Fanaroff & Riley 1974) usually indicated as their “misaligned population”.

Key words: polarization – BL Lacertae objects: general – radio continuum: galaxies

1. Introduction

In recent years a great effort has been spent to explain the observed properties of the various classes of radio-loud Active Galactic Nuclei (AGN) (e.g. radio galaxies, quasars and BL Lac objects) in the framework of Unified Schemes (see Urry & Padovani 1995 for a recent review).

In this context, BL Lac objects play a key role because of the evidence that extreme relativistic effects take place in them. These objects are characterized by a flat radio spectrum which steepens at higher frequencies, relatively high optical and radio polarization, rapid variability and an optical continuum with weak or absent emission lines (Urry & Padovani 1995; Kollgaard 1994).

These properties have been interpreted in terms of a relativistic jet closely aligned to the line of sight (hereafter the “beaming model”; see Blandford & Rees 1978; Ghisellini et al. 1993). This model implies the existence of a class of radio sources (hereafter the “misaligned population”) intrinsically identical to BL Lac objects, but with the jets oriented at large angles to the line of sight.

Browne (1983) and Wardle et al. (1984) were the first to propose the low luminosity edge darkened FR I radio galaxies as the most likely candidate for the “misaligned population” of the core dominated BL Lac objects. A straightforward outcome of the beaming model is that all the properties not depending

on orientation should be shared by the BL Lac objects and the misaligned population. Recently while some authors confirm that the majority of the BL Lac objects are projected FR I radio galaxies (Urry & Padovani 1995, and references therein), others suggest that the diffuse radio emission detected around high redshift BL Lac possesses overall properties more consistent with FR II rather than FR I radio galaxies (see e.g. Kollgaard et al. 1992; Murphy et al. 1993).

In the radio domain the luminosity of the extended radio emission and the polarization properties need to be investigated. In fact, while the morphology is distorted by projection effects and a morphological classification could be uncertain, the luminosity of the unbeamed emission is suitable for a direct comparison with the extended emission found in the candidate misaligned population.

Also the investigation of the polarization properties via deep radio observations are important to verify the FRI–BL Lac unification because the observed magnetic field orientation in the kpc-scale jets is not significantly affected by projection and relativistic effects.

To address the problem of the misaligned population of BL Lac objects we observed 28 (see Bondi et al. 1996 for a summary of the observations) out of the 34 BL Lac objects belonging to the 1 Jy sample of Stickel et al. (1991). The observations were carried out with the Very Large Array (VLA) and the Westerbork Synthesis Radio Telescope (WSRT) in order to search for extended radio emission and to obtain kpc-scale polarization images.

These observations were intended to complete the radio information on the 1 Jy RBL sample, already partially investigated by various groups at several wavelengths. Fourteen objects were observed with the VLA in A and B configuration and were chosen among those without good quality, high dynamic range, radio images in literature. All these 14 together with additional 14 objects were observed with the VLA in the D configuration and/or with the WSRT to look for very extended radio halos.

In this paper we present first promising results from the VLA data in A and B configuration.

A detailed analysis of the whole dataset and a specific discussion of the importance of these new observations in the con-

Table 1. Columns 1 through 6 show: source name, redshift, radio power at 1.4 GHz of the extended emission, percentage of polarization and E-vector position angle in the extended emission (typical errors of 0.1 – 0.2 % and 3 degrees), position angle of the projected magnetic field with respect to the direction of the jet (errors are around 5-10 degrees). The position where the polarization parameters are calculated is shown with a cross in each image and corresponds to the location of the maximum brightness of polarized emission out of the nucleus. The frequency and array configuration at which the quantities presented here are derived for each object is indicated in the caption of the corresponding figure. The redshift of 1147+245 is unknown; the median value for the redshift distribution of the 1 Jy sample has been used for this object.

Source name	z	$P_{1.4}$ $\times 10^{24} W/Hz$	$\%_e$	χ_e deg.	P.A. _B deg.
0954 + 658	0.367	2.3	14.7	−88	+14
1147 + 245	(0.5)	12.8	1.0	+82	+6
1514 – 241	0.049	0.3	11.7	−19	−11
1807 + 698	0.051	2.7	21.2	+6	+39
2131 – 021	0.557	30.5	8.9	+66	+14
2240 – 260	0.774	220.5	12.9	−44	−12

text of the Unification Schemes for BL Lac objects will be presented in forthcoming papers.

Throughout this paper we use $H_0 = 100 \text{ km s}^{-1} \text{ Mpc}^{-1}$ and $q_0 = 0.5$.

2. Observations and data reduction

We present here a subset of the VLA A-array data at L and X bands and of the B-array at L band showing the polarization properties of six sources (Table 1). These have been selected among the observed objects as those clearly showing a polarized jet.

The data reduction has been done in the standard way using the NRAO Astronomical Image Processing System (AIPS). We used 3C286 to calibrate the absolute flux density scale according to the value given by Baars et al. (1977). The radio source 3C286 has been also used to calibrate the polarization position angle. Several iterations of phase self-calibration followed by a final step of amplitude and phase self-calibration were performed to correct for antenna based errors, until the process converged to a stable solution. With this procedure we were able to achieve an rms noise on the cleaned images close to the expected thermal noise. Correction for baseline based errors was not necessary. The polarization images were corrected for the positive bias arising from the Ricean noise.

3. The images

In Fig. 1 we present the radio images for the six objects reported in Table 1. In order to highlight the magnetic field orientation, in the figures we have drawn the B-vectors rather than the E-

vectors as usually found in literature, and the vector length is arbitrary.

By comparing the images at 5 GHz in B configuration and at 1.6/1.4 GHz in A configuration (they have comparable UV coverage and resolution), we found that the Faraday rotation is usually very small. Therefore the orientation of the B vectors in the images presented here is very close to the intrinsic one.

The radio images in Fig. 1 show various features as jets, lobes, halos and, perhaps, even hot-spots. We detected polarized emission not only in the core but, in the majority of the cases, also in the extended features. This permitted us to investigate the magnetic field geometry in regions not affected by relativistic beaming effects.

The percentage of the polarization flux density in the core is usually between 1% and 5%. The polarized flux density in the extended emission (when detected) varies from a few percent to about 50 % across the source. The value given in Table 1 corresponds to the location of maximum brightness (excluding the core) in the polarization image and is indicated with a cross in the images. Here the polarization percentage is typically 10 – 20 %.

We presented these 6 objects because a well defined jet is clearly detected, and significant polarized emission has been revealed along most of the jet length. The observed projected magnetic field runs mostly parallel to the local jet direction. In Table 1 we show the polarization parameters and the difference between the projected B field orientation with respect to the local jet direction at the off nucleus peak position in polarized intensity. Also these numbers confirm that the magnetic field tends to be parallel to the jet direction.

In 1514-241, 1807+698, 2131-021 and 2240-260 the polarization angle drastically change in a “blob” (possibly a hot spot) at the edge of the source.

4. Discussion and conclusions

We can now compare the polarization properties of the extended emission of these six objects with those expected from the Unified Scheme.

In FR I radio sources the magnetic field is parallel to the jet in the vicinity of the core (up to a few kpc), but is dominated by the perpendicular component for the majority of its length (Bridle & Perley 1984, Killeen et al. 1986). On the other hand, in FR II radio sources the magnetic field is parallel to the jet (both on pc and kpc scale), and becomes perpendicular to the source axis in the hot-spots where the magnetic field lines are compressed by a strong shock (Bridle 1986, Bridle et al. 1986, Scheuer 1987).

All the BL Lac objects in Fig. 1 show distinct jet-like features. This is true also for 1147+245 where higher resolution observations (Antonucci et al. 1985) confirm that the polarized southern component is a jet. In all these cases the magnetic field is parallel to the jet axis and follow smoothly any change in direction. In the five sources (0954+658, 1514-241, 1807+698, 2131-021, 2240-260) where we had enough resolution, the jet terminates in a higher brightness and polarized region which

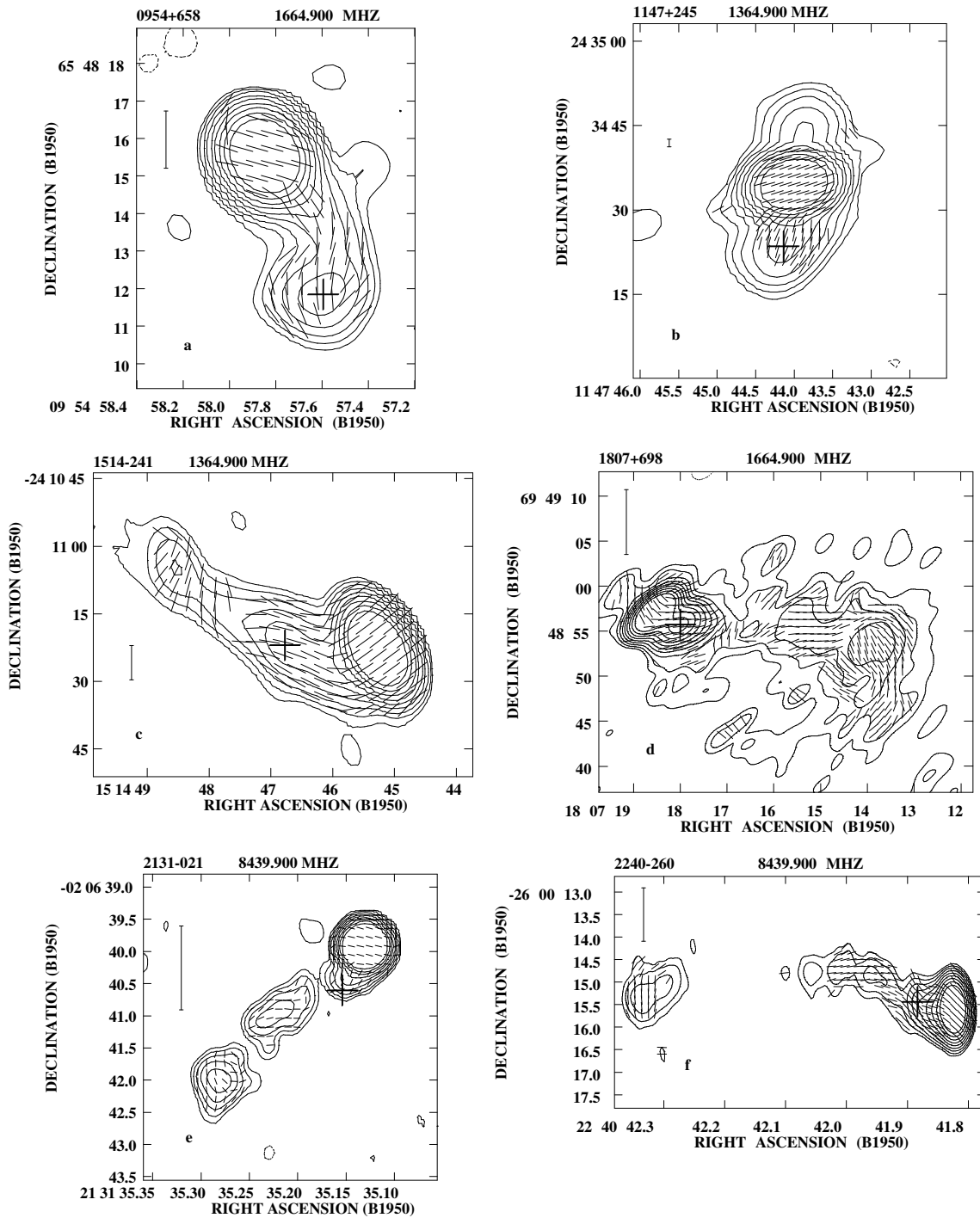


Fig. 1. The contour levels are $-3, 3, 6, 12, 25, 50, 100, 200, 400, 800 \times$ the rms noise. The vertical bar on the left side corresponds to a linear size of 5 Kpc. The vectors superimposed onto the contour levels are of arbitrary length and show the direction of the projected magnetic field. The cross marks the location where the polarization parameters of the extended emission have been measured. (a) 0954 + 658 at 1.66 GHz in A configuration. The restoring beam is 1.2×1 arcsec in P.A. $+35^\circ$. The rms noise on the image is 0.1 mJy. The peak flux is 609 mJy. (b) 1147 + 245 at 1.36 GHz in B configuration. The restoring beam is 7×5 arcsec in P.A. -80° . The rms noise on the image is 0.12 mJy. The peak flux is 715 mJy. (c) 1514 – 241 at 1.36 GHz in B configuration. The restoring beam is 10×6 arcsec in P.A. $+30^\circ$. The rms noise on the image is 0.25 mJy. The peak flux is 1847 mJy. (d) 1807 + 698 at 1.66 GHz in A configuration. The restoring beam is 3×1.5 arcsec in P.A. -48° . The rms noise on the image is 0.15 mJy. The peak flux is 1156 mJy. (e) 2131 – 021 at 8.4 GHz in A configuration. The restoring beam is 0.3×0.3 arcsec. The rms noise on the image is 0.05 mJy. The peak flux is 1597 mJy. (f) 2240 – 260 at 8.4 GHz in A configuration. The restoring beam is 0.6×0.3 arcsec in P.A. $+3^\circ$. The rms noise on the image is 0.1 mJy. The peak flux is 692 mJy.

could be identified with the terminal hot-spot. This hypothesis is reinforced by the orientation of the magnetic field. In 3 sources (1807+698, 2131-021, 2240-260) the magnetic field in the putative hot-spot is transversal as it is expected when a strong shock compresses the field lines. This seems to be the case also for 1514-241 although we note that the change in the magnetic field direction seems to occur still in the jet region. We also note that when a change in magnetic field orientation is observed, it occurs at a larger distance than observed in FR I radio sources if the observed sizes in our objects are foreshortened by projection.

The polarized emission of BL Lac objects shown in Fig. 1 suggests they are FR II radio galaxies viewed end-on. This conclusion is apparently supported by the results obtained from the extended luminosity. Table 1 lists the extended luminosity derived subtracting the core flux density from the total flux density of the source. Only one object (1514-241) has undoubtedly a luminosity of extended emission typical of a FR I radio galaxy. Two objects (0954+658 and 1807+698) have values about the FR I - FR II break ($10^{24.5} - 10^{25}$ W/Hz at 1.4 GHz, Bridle 1984), while three sources have extended luminosities typical of an FR II radio galaxy. On the other hand all the objects shown apart 1147+245 and maybe 1807+698 (which is double lobed in lower resolution images) are one-sided. This suggests that also the extended emission in the majority of the objects shown may be amplified by relativistic boosting, making very difficult any comparison between luminosities.

Several authors have recently debated the BL Lac-FRI Unified Scheme by comparing the host galaxy properties (Wurtz et al. 1996*a*), the clustering properties (Smith et al. 1995; Wurtz et al. 1996*b*), the X-ray properties (Brinkmann et al. 1996), and radio properties (Kollgaard et al. 1992; Murphy et al. 1993; Perlman & Stocke 1993) of different samples of BL Lac objects and FRI/FRII radio galaxies. The results presented here raise new problems to the BL Lac-FRI Unification.

The completion of the analysis of our radio data together with the information already available in literature will allow us to investigate in much greater detail than previously possible the problem of the misaligned population of BL Lac objects and to study whether projection effects may influence the observed polarization properties of jets closely aligned to the line of sight.

Acknowledgements. M.B. and D.D. acknowledge financial support from the the European Union as an EU Fellow under contract ER-BCHBGCT920212. The WSRT is operated by the Netherlands Foundation for Research in Astronomy with the financial support of the of the Netherlands Organization for Scientific Research (NWO). The National Radio Astronomy Observatory is a facility of the National Science Foundation operated under cooperative agreement by Associated Universities, Inc.

References

- Antonucci R.R.J., Ulvestad J.S., 1985, ApJ 294, 158
 Baars J.W., Genzel R., Pauliny-Toth I.I.K., Witzel A., 1977, A&A, 61, 99
 Blandford R.D., and Rees M.J., 1978, in BL Lac Objects, ed. A.M. Wolfe (Univ. of Pittsburgh Press), 328

- Bondi M., Dallacasa D., Stanghellini C., Della Ceca R., 1996, in “Extragalactic radio Sources”, IAU Symp. 175, eds. R.Ekers, C.Fanti, L. Padrielli (Kluwer Publ., Dordrecht), p. 53
 Bridle A.H., Perley R.A., 1984, ARA&A, 22, 319
 Bridle A.H., Perley R.A., Henriksen R.N., 1986, AJ, 92, 534
 Bridle A.H., 1986, Can. J. Phys. 64, 353
 Brinkmann W., Siebert J., Kollgard R.I., Thomas H.-C., 1996, A&A, 313, 356
 Browne I.W.A., 1983, MNRAS, 204,23
 Fanaroff B., Riley J. M., 1974, MNRAS 167, 31
 Ghisellini G., Padovani P., Celotti A., Maraschi L., 1993, ApJ, 407, 65
 Killeen N.E.B., Bicknell G.V., Ekers R.D., 1986, ApJ, 302, 306
 Kollgaard R. I., 1994, Vistas Astron., 38, 29
 Kollgaard R. I., Wardle J.F.C., Roberts D.H., Gabuzda D.C., 1992, AJ, 104, 1687
 Murphy D.W., Browne I.W.A., Perley R.A., 1993, MNRAS, 264, 298
 Perlman E.S., Stocke J.T., 1993, ApJ, 406, 430
 Scheuer P.A.G., 1987 in “Astrophysical Jets and Their Engines”, editor W. Kundt (Reidel, Dordrecht) p. 137
 Stickel M., Padovani P., Urry C.M., Fried J.W., Kühr H., 1991, ApJ, 374, 431
 Urry C.M., Padovani P., 1995, PASP, 107, 803
 Wardle J.F.C., Moore R.L., Angel J.R.P., 1984, ApJ, 279,93
 Wurtz R., Stocke J.T., Yee H.K.C., 1996*a*, ApJ Suppl., 103, 109
 Wurtz R., Stocke J.T., Ellingson E.E., Yee H.K.C., 1996*b*, in preparation